Swelling behaviour of an expansive clay at high suction

V. Mantikos, A. Tsiampousi & J. R. Standing
Department of Civil & Environmental Engineering, Imperial College, London

ABSTRACT: Deep geological disposal designs for nuclear waste often include an engineered barrier to protect the waste canisters and prevent leakage. The long-term safety of the repository relies on studies of the buffer material. Oedometer tests provide values of design parameters for numerical simulations. A newly-developed oedometer with automated suction control is presented to assist in the investigation of the coupled hydro-mechanical-volumetric behaviour of an expansive clay, namely a natural sodium bentonite. The displacement-controlled device was developed to apply suction over a range of 10 MPa to 300 MPa using a divided-flow humidity-generator. The device allows the application of combined stress and suction states, and continuous stress paths of constant volume, stress or suction. The development of the new oedometer is described. Results obtained during the preliminary tests are evaluated through comparison with experimental data from similar tests found in the literature. The current method benefits from continuous control of suction with servo-control of relative humidity using calibrated capacitance hygrometers. The system self-compensates for minor temperature changes and therefore the requirement for thermal insulation is not as crucial as in vapour equilibrium methods.

1 INTRODUCTION

In many countries, including the United Kingdom, deep geological repositories are considered the safest option for disposing radioactive waste (Delage et al., 2010, Holton et al., 2012). The method requires the waste canisters to be encased by an engineered buffer of high plasticity and low permeability. Heavily compacted bentonite satisfies the criteria for a buffer material, including the requirement for maintaining high swelling pressures in the long term (Pusch, 2002, Pusch and Weston, 2015). Bentonite is a clay usually with a high montmorillonite content. Its expansive behaviour and its permeability are strongly related to its void structure and its history in terms of both suction and stress.

Compaction at water contents below optimum results in a double porosity structure. Romero (2013) suggests that changes in microstructure are affected mainly by water content, and subsequently by suction, while loading affects the macrostructure. Further interaction between macro and micro structure has been incorporated within constitutive models (Alonso et al., 1999, Gens et al., 2011) by introducing plastic macroscopic deformations after suction-related yield in the microstructure.

The need for characterisation of the volumetric behaviour of bentonite at high suction and high compression stresses has led researchers to develop oedometers with suction control, capable of applying large loads (> 3 MPa) (Al-Mukhtar et al., 1999, Villar, 1999, Marcial et al., 2002, Lloret et al., 2003, Cuisinier and Masrouri, 2004, Dueck, 2004, Hoffmann et al., 2007, Baille et al., 2010).

While suction control at levels below 1 MPa may be achieved with a number of methods, including osmotic oedometers and axis translation techniques such as the pressure plate apparatus, high levels of suction are mostly achieved using the vapour equilibrium method (Tarantino et al., 2011, Delage et al., 2008). Suction within a sample can be related to relative humidity (RH) using the psychrometric law (Fredlund and Rahardjo, 1993). Instead of using saturated salt solutions, Lu and Likos (2004) used a humidity generator to control RH in a closed system. In the present research, a similar generator (Mantikos et al., 2016) produces an automated humidity control, with the vapour stream being guided across the surfaces of an oedometer sample.

2 EQUIPMENT

2.1 *Test set-up and arrangement of instrumentation*

A new 70-mm diameter oedometer has been designed and fitted with a humidity generator (Mantikos et al., 2016). Vapour at a controlled relative humidity is produced by mixing dry air from the main laboratory compressor with saturated vapour (Figure 1, a,b,c). The mixing ratio is servo-controlled based on the RH measurement (Figure 1, d). Vapour is allowed to flow above and below the sample. An oil trap at the exhaust prevents any reversal in the vapour-flow direction. Sensirion SHT21 capacitance hygrometers record the RH and temperature of the vapour as it enters and leaves the sample (typical RH error is 2% RH between 20% and 80% RH).

Load is applied using a TRI-SCAN 100 loading frame manufactured by VJ Tech and is measured by a 70-kN STALC3 load cell produced by Applied Measurements Ltd. A displacement transducer with a range of 20 mm is used to measure overall displacement. Three miniature LVDTs of ±5-mm range and 0.1-μm resolution are used.

The oedometer ring, base and top cap are made from corrosion resistant steel, AMINOX-AS-1. The height of the ring has been selected to allow for varying sample heights and large initial volume changes during compaction within the cell. Additionally, the thickness of the oedometer ring is 25 mm to ensure radial confinement under high swelling stresses.

The length and diameter of the ram have been designed against buckling resistance. Brass sintered porous stones are used in order to withstand the applied pressures.

O-rings around the ram and below the confining ring further seal the cell. This does lead to potential friction with the cell wall. Use of lubricating silicon grease limits the value of friction to 10-20 kPa, which is acceptable for the range of loads applied.

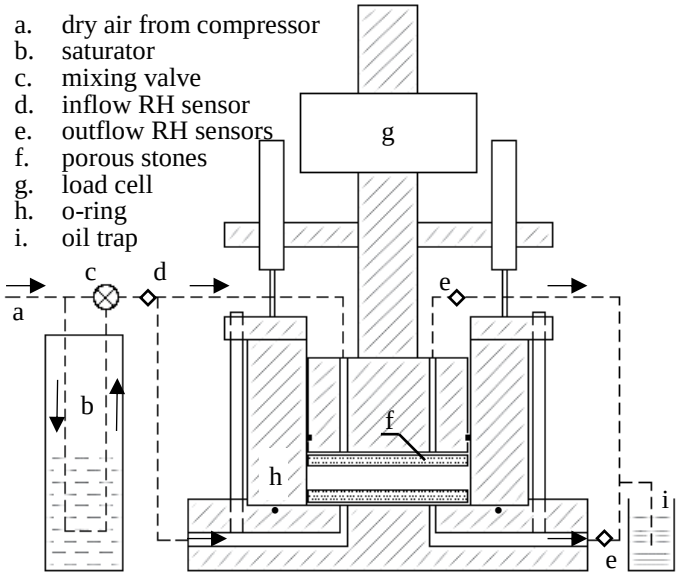

Figure 1. General layout of the finalised RH-controlled oedometer.

3 SOIL TYPE AND TESTING METHOD

3.1 *Index properties*

The soil used in this study is a commercial bentonite, dried, ground and sieved to a yellow-grey clay powder. Throughout this paper it will subsequently be referred to as 'yellow bentonite'. Material properties of this clay are presented in Table 1, along with those of FEBEX and MX80 bentonites, which have been extensively researched as buffer materials (Villar and Lloret, 2008, Wang et al., 2013, Pusch, 2002). The density of the solid particles is ρ_s = 2780 kg/m^3. The Atterberg limits were measured to be w_P = 52% and w_L = 335%, where w_P is the plastic and w_L is the liquid limit.

Heavy dynamic compaction tests (4.5 kg rammer) indicate an optimum water content of w_{opt} = 28% (Figure 2). In terms of soil-water retention curves (SWRC), the curve for the yellow bentonite lies above that of MX80 on both the wetting and drying paths (Figure 3).

Table 1. Index properties of bentonite in present study compared to literature materials (Villar and Lloret, 2008, Wang et al., 2013, Pusch, 2002)

Index property	Yellow bentonite	FEBEX	MX80
Specific gravity	2.78	2.70	2.77
Atterberg limits			
Plastic limit (%)	52	53	53
Liquid limit (%)	335	102	575
Plasticity index (%)	283	49	522

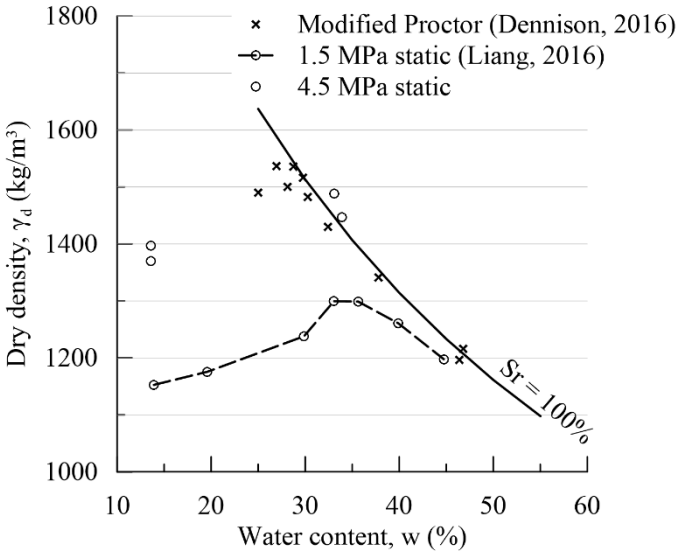

Figure 2. Optimum water content under (a) heavy dynamic compaction (Dennison, 2016), (b) 1.5 MPa static compaction (Liang, 2016) and (c) 4.5 MPa static compaction.

3.2 *Testing method*

The new oedometer is designed to allow vertical movement of the base with a motor drive, relative to a fixed loading ram. The load cell is in line with the

ram, and the top cap is also fixed to it. This fixed connection inhibits any tilting thus allowing for uniform strain on the sample during compaction. The verticality and alignment of the ram is checked and carefully adjusted at the start of each test. Vertical displacements are measured by three LVDTs positioned around the top cap to ensure that no tilting occurs during the test. An additional LVDT measures the distance of the underside of the top cap to the top of the porous stone in contact with the sample through an aperture in the top cap and is used to determine the initial sample height. Deformation measurements are corrected based on compliance tests performed on a stiff dummy sample. Silicon grease was applied on the inside wall of the confining ring prior to placing the soil sample to minimise friction. The porous stones were air dried prior to testing. Filter papers either side of the sample prevent penetration of bentonite particles in the porous stones.

Samples are compacted directly in the oedometer cell at a rate of 0.02 mm/min at ambient RH. Temperature in the laboratory is regulated at 21 ^{0}C ± 0.5 ^{0}C.

In traditional vapour equilibrium methods using salt solutions, the RH of the vapour is very sensitive to temperature fluctuations (Delage et al., 2008). In the new apparatus described here, the RH of the vapour entering the cell is continuously adjusted, maintaining the target value independently of changes in temperature. The vapour is allowed to flow around the sample. Humidity exchange is driven by the potential difference between total suction in the sample and total suction of the circulated vapour as derived from Kelvin's psychrometric law. Attempts to force the vapour through the sample were unsuccessful due to the low air permeability of the compacted sample. Instead, accumulated air pressure developed resulting in an air pocket forming adjacent to the sample. Studies performed within the FORGE (fate of repository gases) project (Sellin, 2014) suggest that below breakthrough pressure, diffusion is the driving gas-transport process and confirm that gas in excess to the gas permeability forms a free phase consolidating the clay.

In the finalised version of the apparatus, the vapour enters the cell at a pressure of approximately 1 kPa. This was found to be sufficient to maintain the flow through the porous stones, around the sample and out of the system. Higher pressures of the dry air entering the system led to increases of the cell pressure measured through the load cell by 25% of the applied air pressure, thus affecting the stress state of the sample. It is possible that a higher flow would accelerate the humidity exchange with the sample, however no significant improvement was observed for the range of entry pressures applied. On the contrary, lower flow allowed for more efficient saturation of the vapour stream and improved the RH control.

RH is controlled at the entry point to the cell and is measured at the exit. Considering a constant flow rate, the humidity exchanged with the sample can be estimated from the difference between the two readings. The measured axial stress at equilibrium is considered to be the swelling pressure.

3.3 *Testing schedule*

The objective of the testing schedule was to prove that the developed equipment can provide reliable swelling pressure measurements under oedometric conditions. In order to achieve this, compressibility tests were performed using both the new and conventional oedometers. The coefficient of volume compressibility, m_v, was calculated for all samples over the linear range of the compression curve at 1.0 MPa (Table 2).

Five samples were prepared. Sample 5001 was compacted in a conventional oedometer while samples 7002, 7003, 7005 and 7006 were compacted in the new oedometer.

Samples 5001, 7002 were prepared at water contents higher than optimum and were sealed for 48 hours prior to compaction. Samples 7003 and 7005 were compacted at hygroscopic water content, below the optimum water content. The suction acting in the samples can be estimated using the primary wetting retention curve (Figure 3). At w = 35%, samples 5001 and 7002 had an estimated initial suction of less than 5 MPa while at w = 14%, samples 7003 and 7005 had an estimated initial suction of 60 MPa. During compression at constant water content, void ratio decreased while the degree of saturation increased. The circulation of vapour at controlled RH limits any potential compression-induced suction change.

Samples 7003, 7005 and 7006 were further subjected to a wetting stage under constant volume. The stiff confining ring and the ram restricted measured deformations to less than 2 nm. Vapour flow through the porous stones was regulated to a target 90% RH, corresponding to a total suction of 10 MPa. The three samples were removed from the cell after different exposure times to investigate the time required for the samples to come to equilibrium (Table 2).

Table 2. Summary of tests.

Sample	5001	7002	7003	7005	7006
Oedometer	conv.	new	new	new	new
Compaction stage					
w (%)	34	33	14	14	14
height (mm)	10.3	15.3	11.9	17.1	16.7
ρ_d (kg/m^3)	1440	1440	1380	1340	1320
m_v (m^2/MN)	0.29	0.27	0.10	0.10	-
e	0.92	0.91	1.05	1.07	1.12
Wetting stage					
duration (days)	-	-	6	15	54
w_f (%)	-	-	18.5	21.4	22.8
p_s (MPa)	-	-	2.23	2.08	1.29

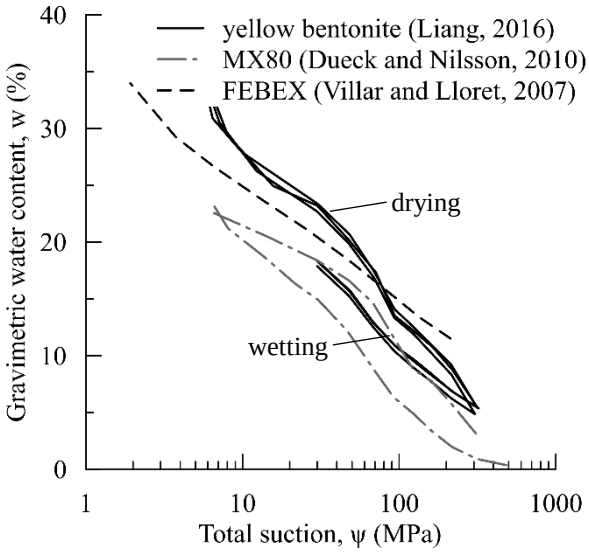

Figure 3. Soil-Water Retenion Curves of yellow bentonite, FEBEX and MX80 (Liang, 2016, Villar and Lloret, 2007, Dueck and Nilsson, 2010)

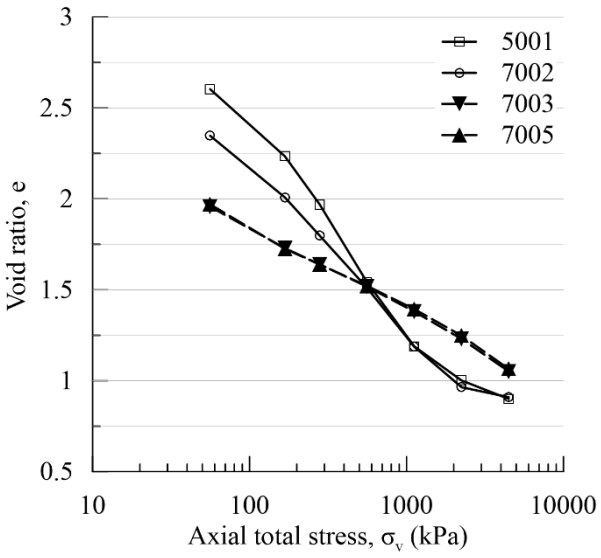

Figure 4. Compression of four bentonite samples.

4 RESULTS

The compression curves of the four samples tested are presented in Figure 4.

Bentonite powder was loosely placed in the cell, resulting in an open structure with high initial void ratio. The sample compacted in the conventional oedometer (5001) had a higher initial void ratio than the corresponding sample in the new oedometer (7002). The two samples started from an initially partly saturated state (S_r = 30%-35%) and reached S_r = 100% by the end of compression (Figure 4).

Samples 5001 and 7002 exhibit three distinctive ranges of compressibility, while samples 7003 and 7005 have a linear compression line.

The initial increase in compressibility is a result of suction reduction due to compression and reduction of macroscopic void ratio, resulting in an apparent pre-consolidation stress. Baille et al. (2010) and Marcial et al. (2002) interpreted the second change as a transition from compression of the inter-particle void space to compression of the microstructure. Both authors report bilinear compression lines for saturated bentonite with compressibility reducing after a threshold of approximately 1 MPa.

Samples 7003 and 7005 present a stiffer behaviour which can be attributed to the higher initial suction. The transition between macro- and microstructure is not present over the examined stress range, as the material remains unsaturated at the end of compression (S_r = 50%-55%).

Samples 7003, 7005 and 7006 were subjected to a high RH, under constant volume conditions. Comparison of the final water content of the samples (Table 2) indicates that sample 7003 has absorbed significantly less water after 6 days than sample 7005 after 15 days, indicating that equilibrium was not reached.

Equilibrium is evaluated during the test by monitoring axial total stress and the RH measured as the vapour leaved the sample. The total stress acting on the soil is not a sufficient indicator of equilibrium as compacted expansive clays show multiple peaks in swelling pressure during a single step of wetting. Studies have associated this phenomenon with double structure (Lloret et al., 2003, Gens et al., 2011). The first drop represents collapse of macrostructure on the Load-Collapse (LC) curve. It is gradual, as the microstructure continuous to swell. Once the macrostructure has fully collapsed, the total stress increases as the microstructure attempts to swell.

Figure 5 presents the evolution of axial stress during the wetting stage for sample 7005. The swelling stress at this suction level is taken to be the stress at equilibrium.

Sample 7005 presents a single peak in swelling pressure of 3.2 MPa after 24 hours of wetting (Figure 5a), before dropping gradually to 2.1 MPa. As suction reduces and load increases, the stress state moves towards the LC yield curve. When the LC is reached, the stress state will move along it, reducing load while suction reduces further. At the time of the first peak, the RH of the vapour leaving the sample (equivalent to 30 MPa total suction) is still significantly lower than the target RH (equivalent to 14 MPa total suction), indicating that the sample is still absorbing water from the vapour flow. Suction can be seen to still be reducing by the end of the second week of wetting in Figure 5b. No further increase in stress is observed for this material, suggesting that the stress at equilibrium is indeed the swelling pressure of the microstructure.

The initial water content of 14% corresponds to a relative humidity of 65% according to the SWRC. The moisture absorbed by the sample can be calculated considering the difference between the RH of the vapour entering and leaving the sample. Using simple measurements, the vapour flow was measured

to be approximately Q = 0.58 litres/min. The calculated water retained by the system, including sample, porous stones and filter papers, is 6.8 g for sample 7005 and 7.2 g for sample 7006. The actual absorbed water measured upon dismantling the sample was 7.0 g and 7.9 g respectively.

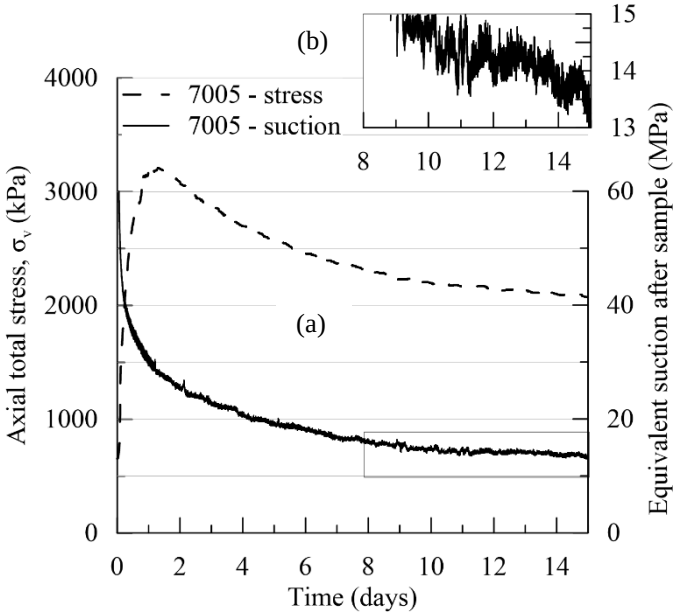

Figure 5. Swelling stress evolution during wetting and total suction measurement after cell, with focus on stability of suction measurements.

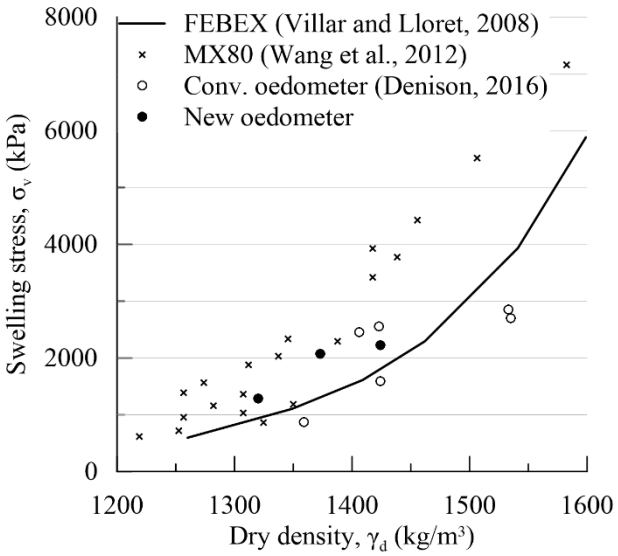

Figure 6. Swelling pressure as a function of dry density. Logarithmic relationships for FEBEX and MX80 bentonite for comparison. (Villar and Lloret, 2008, Wang et al., 2012)

The underestimation of the mass of water absorbed for both samples is a consequence of the accuracy of RH measurement in conjunction with the assumptions made in calculating the mass of water exchanged per time increment. Changes in the water content of the sample were calculated by comparing the water mass in the vapour entering and leaving the sample using thermodynamic principles.

Figure 5b focuses on the fluctuation of suction measurements during the second week of wetting for sample 7005. According to the psychrometric law, at 90% RH, the observed fluctuation of 0.3% RH represents a change of ±0.5 MPa of suction. The typical RH error of an individual SHT21 sensor at 90% RH is 2.5% RH, or ±3.7 MPa. However, the error between sensors has been consistently less than ±0.5% RH. As the calculations are based on the difference between inflow and outflow, the corresponding uncertainty in water mass change accounts to ±0.14 g/day. It is evident that this approach is not applicable near equilibrium (when RH error > RH_{in} - RH_{out}), where the uncertainty is expected to be greater than the daily change. Therefore, the measurement of RH alone cannot provide a fully reliable means of identifying when the sample has reached equilibrium. Ideally there should be another independent measurement, such as the swelling pressure.

The ultimate axial (swelling) stress, i.e. at equilibrium, for each corresponding dry density is plotted in Figure 6. The equilibrium stress is considered to be a more appropriate means of describing the swelling pressure for the long-term behaviour of the material. The swelling pressures calculated by Dennison (2016) on the same yellow bentonite using conventional oedometers is also shown in Figure 6 for comparison. Dennison was measuring peak stress while saturating the samples with water. While his method would be expected to result in higher swelling pressures than the ultimate pressures of the present study, the higher pressures measured with the new oedometer can be attributed to the robustness of the ring and the more effective volume control. The results are reasonable, plotting close to FEBEX and MX80 bentonites, suggesting that there were no adverse effects from using the new oedometer.

5 CONCLUSIONS

The newly developed oedometer uses the vapour transfer method for controlling suction. An automated humidity generator produces vapour over a range of 10 - 300 MPa of suction, with a standard deviation of 0.3% RH. Relative humidity of the vapour both entering and leaving the sample is measured with capacitance hygrometers. Relative humidity readings before and after the cell allow for an estimation of water exchange between the vapour and the sample.

The vapour transfer method presented here benefits over traditional salt solution methods in the sense that RH can be applied over a continuous range, and in that the recorded value is independent of temperature fluctuations. However, measurements with the new system of suction below 30 MPa should be treated with caution, as the uncertainty related to the accuracy of the hygrometers increases significantly.

Results from compression and swelling tests on the yellow bentonite are consistent with those obtained using conventional oedometers. The bentonite has similar retention properties and swelling pressures to

MX80 bentonite and exhibits key characteristics of double structure.

6 ACKNOWLEDGEMENTS

The first author is supported by a Skempton scholarship and the project is partly funded by Radioactive Waste Management ltd (RWM). The equipment has been developed thanks to the engineering skills of the team of technicians in the Soil Mechanics Laboratory of Imperial College, including Steve Ackerley and Duncan Parker. Part of the results presented were carried out by Thomas Dennison and Jicheng Liang as part of their MSc theses. Special thanks to Dr. David Taborda for his input and support in designing the equipment.

7 REFERENCES

Al-Mukhtar, M., Qi, Y., Alcover, J. F. & Bergaya, F. 1999. Oedometric and water-retention behavior of highly compacted unsaturated smectites. *Canadian geotechnical journal* 36(4)**:** 675-684.

Alonso, E. E., Vaunat, J. & Gens, A. 1999. Modelling the mechanical behaviour of expansive clays. *Engineering Geology* 54(1-2)**:** 177-183.

Baille, W., Tripathy, S. & Schanz, T. 2010. Swelling pressures and one-dimensional compressibility behaviour of bentonite at large pressures. *Applied Clay Science* 48(3)**:** 324-333.

Cuisinier, O. & Masrouri, F. 2004. Testing the hydromechanical behavior of a compacted swelling soil. *Geotechnical Testing Journal* 27(6)**:** 598-606.

Delage, P., Cui, Y.-J. & Tang, A.-M. 2010. Clays in radioactive waste disposal. *Journal of Rock Mechanics and Geotechnical Engineering* 2(2)**:** 111-123.

Delage, P., Romero, E. & Tarantino, A. 2008. Recent developments in the techniques of controlling and measuring suction in unsaturated soils. *Unsaturated Soils: Advances in Geo-Engineering***:** 33-52.

Dennison, T. D. 2016. Experimental Investigation in to the Swelling Potential of Dynamically-Compacted Bentonite. MSc Dissertation, Imperial College London.

Dueck, A. 2004. Hydro-mechanical properties of a water unsaturated sodium bentonite. Laboratory study and theoretical interpretation. PhD, Lund University.

Dueck, A. & Nilsson, U. 2010. Thermo-Hydro-Mechanical properties of MX-80, Results from advanced laboratory tests. *Svensk Kärnbränslehantering AB*. SKB TR 10-55.

Fredlund, D. G. & Rahardjo, H. 1993. Soil mechanics for unsaturated soils, John Wiley & Sons.

Gens, A., Sanchez, M. & Vallejan, B. 2011. Published. Generalized plasticity for geomaterials with double structure. *11th International Conference on Computational Plasticity, COMPLAS XI*, September 7 - September 9, 2011, Barcelona, Spain. International Center for Numerical Methods in Engineering: 32-41.

Hoffmann, C., Alonso, E. E. & Romero, E. 2007. Hydro-mechanical behaviour of bentonite pellet mixtures. *Physics and Chemistry of the Earth, Parts A/B/C* 32(8–14)**:** 832-849.

Holton, D., Baxter, S. & Hoch, A. R. 2012. Modelling coupled processes in bentonite: recent results from the UK's contribution to the Äspö EBS Task Force. *Mineralogical Magazine* 76(8)**:** 3033-3043.

Liang, J. 2016. Measurement of the soil-water retention curve of bentonite. MSc Dissertation, Imperial College London.

Lloret, A., Villar, M. V., Sanchez, M., Gens, A., Pintado, X. & Alonso, E. E. 2003. Mechanical behaviour of heavily compacted bentonite under high suction changes. *Geotechnique* 53(1)**:** 27-40.

Lu, N. & Likos, W. J. 2004. Unsaturated Soil Mechanics, Hoboken, New Jersey, John Wiley & Sons.

Mantikos, V., Ackerley, S., Kirkham, A., Tsiampousi, A., Taborda, D. M. G. & Standing, J. 2016. Published. Investigating soil water retention characteristics at high suctions using relative humidity control. *3rd European Conference on Unsaturated Soils, E-UNSAT 2016*, 12-14 September, 2016, Paris, France. E3S Web Conf.: 10007.

Marcial, D., Delage, P. & Cui Jun, Y. 2002. On the high stress compression of bentonites. *Canadian Geotechnical Journal* 39(4)**:** 812-820.

Pusch, R. 2002. The Buffer and the Backfil Handbook. Part 2: Materials and techniques. *SKB*.

Pusch, R. & Weston, R. 2015. Superior techniques for disposal of highly radioactive waste (HLW). *Environmental Earth Sciences* 73(9)**:** 5219-5231.

Romero, E. 2013. A microstructural insight into compacted clayey soils and their hydraulic properties. *Engineering Geology* 165(Supplement C)**:** 3-19.

Sellin, Patrick (editor). 2014. Experiments and modelling on the behaviour of EBS. *FORGE*. Report D3.38. 426pp.

Tarantino, A., Gallipoli, D., Augarde, C. E., De Gennaro, C. E., Gomez-Espina, R., Laloui, L., Mancuso, C., El Mountassir, G., Munoz, J. J., Pereira, J. M., Peron, H., Pisoni, G., Romero, E., Raveendiraraj, A., Rojas, J. C., Toll, D. G., Tombolato, S. & Wheeler, S. J. 2011. Benchmark of experimental techniques for measuring and controlling suction. *Géotechnique* 61(4)**:** 303-312.

Villar, M. V. 1999. Investigation of the behaviour of bentonite by means of suction-controlled oedometer tests. *Engineering Geology* 54(1-2)**:** 67-73.

Villar, M. V. & Lloret, A. 2007. Dismantling of the first section of the FEBEX in situ test: THM laboratory tests on the bentonite blocks retrieved. *Physics and Chemistry of the Earth, Parts A/B/C* 32(8–14)**:** 716-729.

Villar, M. V. & Lloret, A. 2008. Influence of dry density and water content on the swelling of a compacted bentonite. *Applied Clay Science* 39(1-2)**:** 38-49.

Wang, Q., Tang, A. M., Cui, Y.-J., Barnichon, J.-D. & Ye, W.-M. 2013. A comparative study on the hydro-mechanical behavior of compacted bentonite/sand plug based on laboratory and field infiltration tests. *Engineering Geology* 162(Supplement C)**:** 79-87.

Wang, Q., Tang, A. M., Cui, Y.-J., Delage, P. & Gatmiri, B. 2012. Experimental study on the swelling behaviour of bentonite/claystone mixture. *Engineering Geology* 124(1)**:** 59-66.